Received January 5, 2014; Accepted March 18, 2014

International Journal of Asia Digital Art&Design

A Color Palette based Interface for Biological Iridescences Rendering

Park Junmin
Graduate School of Design, Kyushu University
tuna.pacific@gmail.com

Tsuruno Reiji
Faculty of Design, Kyushu University
tsuruno@design.kyushu-u.ac.jp

Abstract

Iridescence is an optical phenomenon of surfaces in which hue changes in proportion to the angles of observation and illumination. Iridescent colors can be observed on many biological objects including morpho butterflies and Japanese jewel beetles. While ordinary colors are induced by pigments in surface, the iridescent colors are caused by interference of light due to microstructure covering the objects. To render iridescences in computer graphics, users need to consider a lot of physical parameters such as index of refraction or film layer thickness. However, in such input systems, users are difficult to predict rendering results since iridescence is affected by combination of those many physical factors. In this paper, we propose a color palette based interface for biological iridescences rendering, with which users can pass information for rendering iridescences to system by picking colors instead of by inputting physical data of surface. Incident angle dependency of reflectance spectrum is studied in details to achieve physically sound simulation and color picking user interface. We also evaluated our system through rendering results(of morpho butterflies and Japanese jewel beetles) and user study in the latter half of this article.

Keywords: iridescence color, spectral rendering, user interface

1 Introduction

Iridescence is an optical phenomenon of surfaces in which hue changes in proportion to the angles of observation and illumination [1]. We can easily find iridescence colors on objects such as compact discs, bubbles and also on animals such as morpho butterflies and Japanese jewel beetles. Iridescences are caused by physical phenomena including thin film interference, multilayer interference, diffraction gratings, photonic crystals and light scattering [2] (Figure 1). Among those mechanisms, iridescence treated in our system is limited to the one due to biological multilayer systems which are found in morpho butterflies, Japanese jewel beetles, neon tetra and many other animals (Figure 2).

Generally, to render iridescences in computer graphics, users need to consider a lot of physical parameters of surface such as index of refraction or film layer thickness. However, in such input systems, users are difficult to predict rendering results since iridescence is affected by combination of those many physical factors.

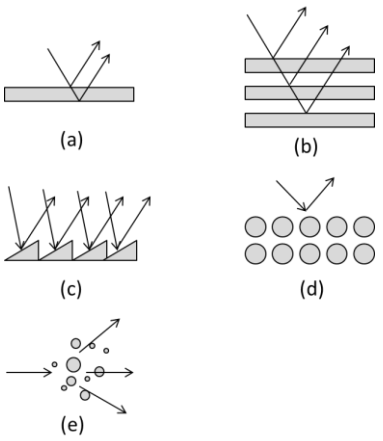

Figure 1 Various optical phenomena causing iridescences
(a)-(e) are thin film interference, multilayer interference, diffraction gratings, photonic crystals and light scattering respectively.

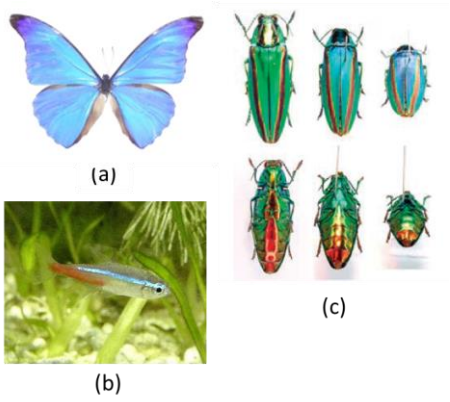

Figure 2 Examples of iridescences caused by multilayer structures
(a)-(c) are morpho butterfly(M. rhetenor), neon tetra and Japanese jewel beetle respectively[3,4].

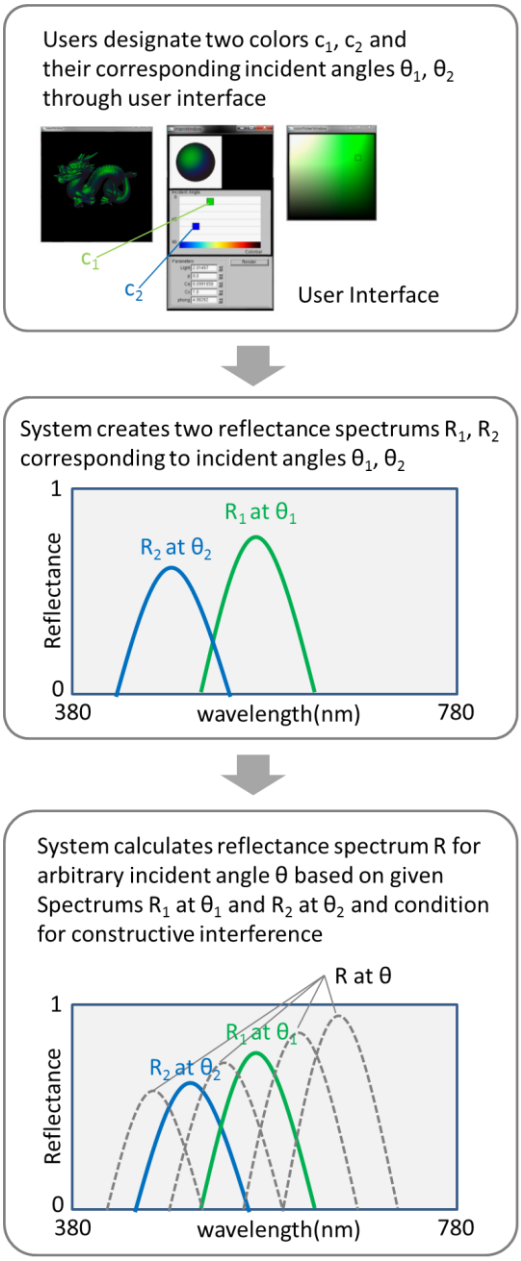

Figure 3 The process to calculate reflectance spectrums for iridescences rendering from user inputs

Once again, the characteristics of iridescence color is laid on its color changes in proportion to the incident angles of light. Thus, the aim of this article is to achieve a system that calculates correspondence between reflectance spectrum(relationship between reflectance spectrum and color is described in Appendix) and its incident angle with enhanced usability. We propose a user interface that allows users to input information for rendering iridescences by designating colors and their incident angles instead of by considering physical parameters. From the information given by users, two reflectance spectrums for corresponding incident angles are defined in our system. Then, correspondence between reflectance spectrums and incident angles is calculated based on the two spectrums and equation of constructive interference, which leads to full information for iridescence color rendering. These processes are summarized in Figure 3.

Section 2 reviews previous works on iridescence rendering in computer graphics. Section 3 describes methods to model reflectance spectrums and calculates correspondence between the spectrums and incident angles. Section 4 presents user interface and section 5 describes evaluation on our system through reflectance spectrum comparison, rendering results and user study. Section 6 concludes this article and discusses the limitation of our methods.

2 Related Work

Several methods have been developed to represent iridescence phenomenon. Hirayama et al.[5] proposed an rendering model for iridescent colors appearing on natural objects through the use of a hypertexture. Hirayama et al.[6] also developed an accurate illumination model for objects coated with multilayer films considering composite reflectance and transmittance. Stam[7] proposed a new class of reflection models for metallic surfaces that handle the effects of diffraction. Gondek et al.[8] developed a method that represents interference of light due to paint and thin film by using a Monte Carlo ray tracer to cast rays into a surface. Iwasawa et al.[9] proposed rendering methods for models with complicated micro structures considering diffraction, light scattering and anisotropy. Nagata et al.[10] developed a rendering model for pearls by calculating multiple reflection in spherical bodies. Sun [11] proposed a model that handles rendering of biological objects by analytical calculation.

As a whole, previous studies have focused on how to simulate iridescences realistically and with these efforts this beautiful phenomenon can be reproduced close to real one by computer graphics nowadays. On the other hand, there is no research that handles user interfaces that assist users to input rendering information to system intuitively in this field.

3 Iridescence Model

In this section, we discuss how to model reflectance spectrums of biological multilayer systems and how to calculate correspondence between reflectance spectrums and incident angles. The method to designate colors(or spectrums) and their corresponding incident angles will be treated in section 4 for easy understanding of this article.

3.1 Reflectance Spectrum of Biological Multilayer System

In multilayer systems(figure 4), the condition for constructive interference is expressed as[2]

$$2(n_A d_A \cos\theta_A + n_B d_B \cos\theta_B) = m\lambda \qquad (3.1.1)$$

where n_A, n_B, d_A, d_B, θ_A, θ_B refer to index of refraction, layer thickness and refractive angle of layer A and B respectively λ is wavelength of incident ray and m is integer greater than 0. In most cases, multilayer system of biological objects satisfy equation (3.1.1) with the range of $380 < \lambda < 780$(namely, the range of visible wavelength of light) when m equals 1[12].

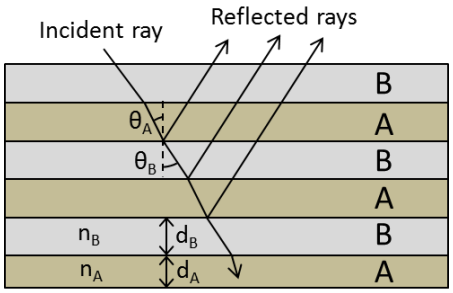

Figure 4 Multilayer system

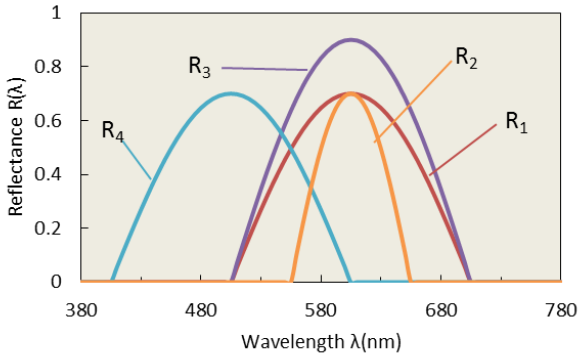

Figure 5 Shapes of reflectance spectrum based on equation (3.1.2)
The values of (λ_{peak}, w, h) for spectrum R_1, R_2, R_3, R_4 are (600, 200, 0.7), (600, 100, 0.7), (600, 200, 0.9), (500, 200, 0.7), respectively.

This implies that reflectance spectrum shows one peak in visible wavelength region, therefore, we define the shape of reflectance spectrum R as following expression:

$$R(\lambda_{peak}, w, h, \lambda)=h \cdot \cos((n/w)(\lambda-\lambda_{peak})) \quad (\text{if } \lambda_{peak}-w/2<\lambda<\lambda_{peak}+w/2)$$
$$R(\lambda_{peak}, w, h, \lambda)=0 \quad (\text{if } \lambda<\lambda_{peak}-w/2 \text{ or } \lambda_{peak}+w/2<\lambda) \qquad (3.1.2)$$

where w, h, λ_{peak} are width, height and peak wavelength of spectrum respectively. These 3 factors define the shape of reflectance spectrum as shown in Figure 5 and are provided through color palette which will be discussed in section 4 in detail.

3.2 Correspondence between Reflectance Spectrum and Incident Angle

Reflectance spectrum R assumed in section 3.1 doesn't include incident angle terms that are necessary to explain iridescence`s behavior. Therefore, we define correspondence between reflectance spectrum and incident angle here. In other words, λ_{peak}, w, h of equation (3.1.2) will be described in terms of incident angle in this section.

From the discussion in section 3.1, the condition for constructive interference in biological multilayer system is expressed as

$$\lambda_{peak}=2(n_A d_A \cos\theta_A+n_B d_B \cos\theta_B) \qquad (3.2.1)$$

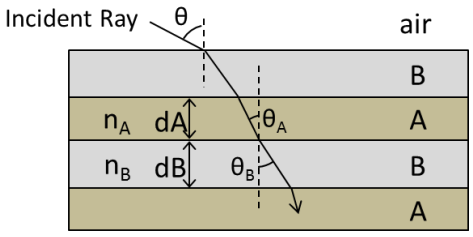

Figure 6 Multilayer structure above which air layer exists
θ is incident angle from air layer.

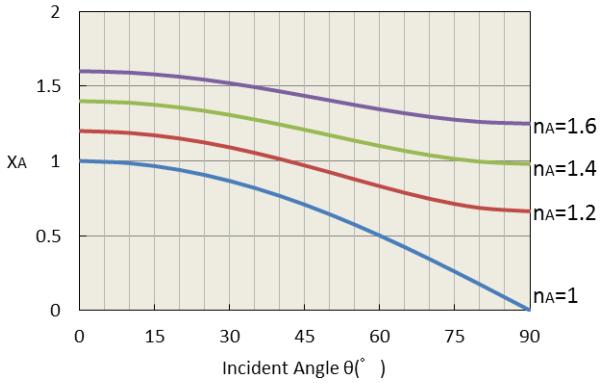

Figure 7 Curves of X_A for different values of n_A between 1 and 2
n_A values of the curves are 1, 1.2, 1.4, 1.6 respectively from bottom to top.

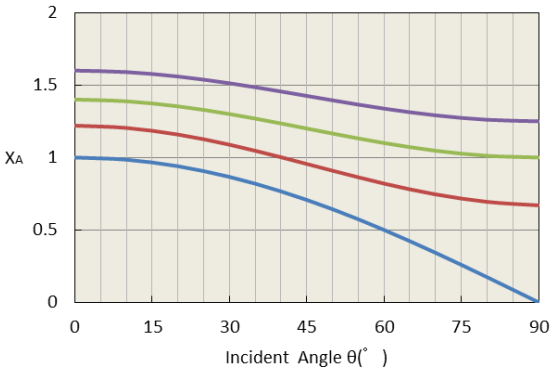

Figure 8 Curves of X_A constructed from linear combination of $\cos^2\theta$, $\cos\theta$ and a constant.
(l, m, n) values of the curves are (0, 1, 0), (0.5, 0.05, 0.67), (0.4, 0, 1), (0.35, 0, 1.25) respectively from bottom to top.

It is natural to assume that the region above multilayer is air as shown in Figure 6, and in such case, the following relationship (3.2.2) is derived according to Snell`s Law[13],.

$$n_A \sin\theta_A = n_B \sin\theta_B = 1 \cdot \sin\theta \tag{3.2.2}$$

where θ is incident angle from air layer. Given equations (3.2.1) and (3.2.2), then

$$\lambda_{peak} = 2(d_A X_A + d_B X_B)$$
$$(X_A = (n_A^2 - \sin^2\theta)^{1/2},\ X_B = (n_B^2 - \sin^2\theta)^{1/2}) \tag{3.2.3}$$

In figure 7, we plot the curves of X_A for different values of n_A between 1 and 2. The curve is cosine when n_A equals 1, but for other values of n_A, curves are S-shaped. To simplify X_A that is expressed with root term, we assume X_A as linear combination of $\cos^2\theta$, $\cos\theta$ and a constant:

$$X_A = l\cos^2\theta + m\cos\theta + n \tag{3.2.4}$$

where l, m are coefficients and n is .a constant. In figure 8, the curves of X_A of equation (3.2.4) are plotted with (l, m, n) values, (0, 1, 0), (0.5, 0.05, 0.67), (0.4, 0, 1), (0.35, 0, 1.25) respectively from bottom to top from the plotted curves, it is proved that X_A of new form is sufficiently similar to the original equation by selecting appropriate values of l, m, n.

Since X_B can be also described by equation (3.2.4), applying X_A, X_B of new forms to equation (3.2.3), the following equation (3.2.5) is derived:

$$\lambda_{peak} = k(p\cos^2\theta + (1-p)\cos\theta) + q \tag{3.2.5}$$

where k, p are coefficients and q is a constant. Coefficient p(0~1) is a parameter that determines the shape of $\lambda_{peak}(\theta)$ between cosine shape(p=0) and s shape(p=1) and this will be inputted by users.

Given two pairs of peak wavelength and its corresponding incident angle, namely, (λ_{peak1}, θ_1), (λ_{peak2}, θ_2), the following relationships are derived from equation (3.2.5):

$$\lambda_{peak1} = kY_1 + q \quad (Y_1 = p\cos^2\theta_1 + (1-p)\cos\theta_1) \tag{3.2.6}$$
$$\lambda_{peak2} = kY_2 + q \quad (Y_2 = p\cos^2\theta_2 + (1-p)\cos\theta_2) \tag{3.2.7}$$

Solving equation (3.2.6) and (3.2.7), then

$$k = (\lambda_{peak1} - \lambda_{peak2})/(Y_1 - Y_2) \tag{3.2.8}$$
$$q = (\lambda_{peak1} Y_2 - \lambda_{peak2} Y_1)/(Y_2 - Y_1) \tag{3.2.9}$$

Applying equation (3.2.8) and (3.2.9) to equation (3.2.5), the final relationship between incident angle θ and corresponding peak wavelength λ_{peak} is derived (note Figure 9).

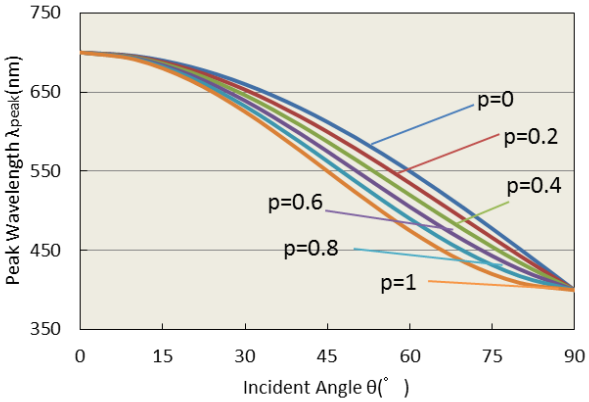

Figure 9 Relationship between peak wavelength λ_{peak} and corresponding incident angle θ, given (700, 0) and (400, 90) for values of (λ_{peak1}, θ_1) and (λ_{peak2}, θ_2)
p values of the curves are 1, 0.8, 0.6, 0.4, 0.2, 0 respectively from bottom to top. As incident angle increases, peak wavelength decreases, which is general characteristics of reflectance spectrum caused by multilayer structures.

For the remaining factors of equation (3.1.2), w, h, we empirically define that those are linear functions of λ_{peak}.

From the discussion above, given reflectance spectrum R_1(=R(λ_{peak1}, w_1, h_1, λ)) and R_2(=R(λ_{peak2}, w_2, h_2, λ)) corresponding to incident angle θ_1, θ_2 respectively, reflectance R for arbitrary incident angle θ is expressed as

$$R = R(\lambda_{peak}, w, h, \lambda) \tag{3.2.10}$$
$$h = (\lambda_{peak} - \lambda_{peak1})(h_2 - h_1)/(\lambda_{peak2} - \lambda_{peak1}) + h_1 \tag{3.2.11}$$
$$w = (\lambda_{peak} - \lambda_{peak1})(w_2 - w_1)/(\lambda_{peak2} - \lambda_{peak1}) + w_1 \tag{3.2.12}$$
$$\lambda_{peak} = k(p\cos^2\theta + (1-p)\cos\theta) + q \tag{3.2.13}$$

k, q in equation (3.2.13) can be calculated from equation (3.2.8) and (3.2.9). Note that now h, w and λ_{peak} are all functions of incident angle θ.

4 User Interface

User interface consists of 3 parts, output window, parameter setting window, color palette window as shown in Figure 10. In this section, we first look into each part of user interface and then describe how to use to render iridescence colors.

4.1 Output window(Figure 10(a))

Rendering results are drawn here based on the information from parameter setting window and color palette.

4.2 Parameter setting window(Figure 10(b))

In this part, rendering parameters for iridescences such as the value of p(which doesn't affect rendering result so much) and two pairs of peak wavelength and its corresponding incident angle, (λ_{peak1}, θ_1) and (λ_{peak2}, θ_2) are designated by users. The region where these peak wavelengths and incident angles are inputted is λ_{peak}-θ plane(Figure 11). In the plane, x-axis(380~780) and y-axis(90~0) represents incident angle θ and peak wavelength λ_{peak}, respectively. There are two mova-

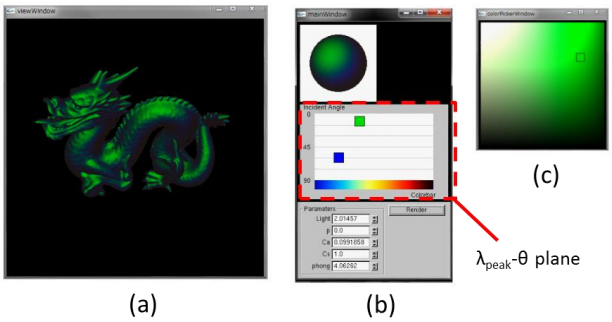

Figure 10 User interface
(a)-(c) are output window, parameter setting window and color palette window respectively.

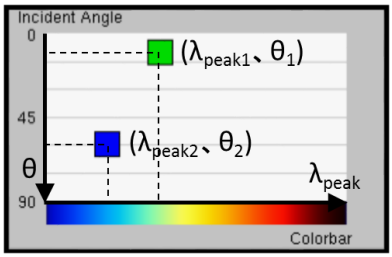

Figure 11 λ_{peak}-θ plane

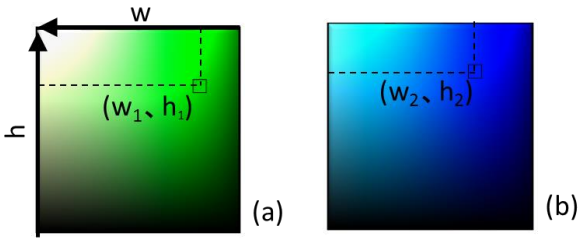

Figure 12 Color palette
(a),(b) are palettes when squares of (λ_{peak1}, θ_1) and (λ_{peak2}, θ_2) are selected on λ_{peak}-θ plane respectively.

ble squares, and their colors are calculated from reflectance spectrum R_1 and R_2(Note Appendix). Based on the coordinates of the squares, the values of (λ_{peak1}, θ_1) for R_1 and (λ_{peak2}, θ_2) for R_2 are determined

4.3 Color palette window(Figure 10(c))

In this part, users set spectrum height h_i and spectrum width w_i for R_i when given λ_{peaki} and θ_i (i=1, 2)(Figure 12). In color palette, x-axis(0~1) and y-axis(400~40) represent w and h respectively. The color of coordinate (w, h) in the palette corresponds to color of spectrum $R_i(\lambda_{peaki}, w_i, h_i, \lambda)$. Therefore, right side of the palette corresponds to spectrum with narrow width (Note that saturation is high and brightness is low in right side of the palette). The upper side of the palette refers to spectrum whose reflectance is high (Note that upper region of the palette is bright). There is one controllable square, and with its coordinate the values of w_i and h_i are determined.

4.4 User input flow

1. First, users designate hue of the color and its incident angle of purpose by moving one of the squares on λ_{peak}-θ plane in parameter setting window. As a result, peak wavelength λ_{peak1}, incident angle θ_1 for reflectance spectrum R_1 is determined.

2. After that, users control brightness and saturation by moving a square on color palette, which determines height h_1 and width w_1 for R_1.

3. λ_{peak2}, h_2, w_2 for R_2 and θ_2 are determined by repeating flow 1, 2 above again with the other square on λ_{peak}-θ plane.

4. Based on user input above, $R(\lambda_{peak}, w, h, \lambda)$ is calculated for arbitrary incident angle θ in the system.

5 Evaluation

5.1 Reflectance Spectrum Comparison

Reflectance spectrum R for arbitrary incident angle θ is calculated based on user inputted spectrums R_1 and R_2 in our system as discussed in section 3.2, Here, the calculated correspondence between R and θ by our method is compared with published reflectance spectrum data of morpho butterflies and Japanese jewel beetle for validation.

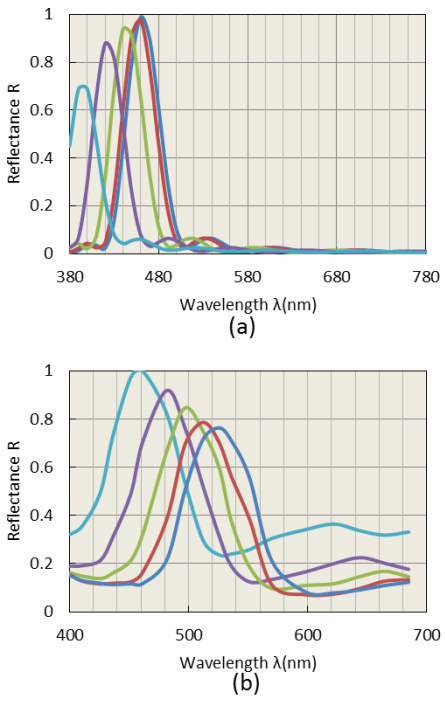

Figure 13 Reflectance spectrum and its incident angle dependency(from reference data[11,14])
(a)-reflectance spectrum of morpho butterfly. From right to left, spectrums correspond to incident angles 0°, 10°, 20°, 30°, 40° respectively.
(b)-reflectance spectrum of Japanese jewel beetle. From right to left, spectrums correspond to incident angles 20°, 30°, 40°, 50°, 60° respectively.

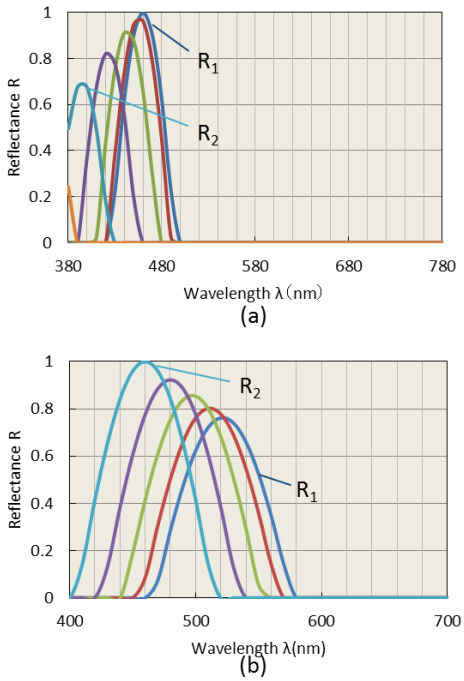

Figure 14 Reflectance spectrum and its incident angle dependency(calculated by our method)
(a)-reflectance spectrum of morpho butterfly. From right to left, spectrums correspond to incident angles 0°, 10°, 20°, 30°, 40° respectively. R_1 and R_2 are selected as R(460, 70, 1, λ) at incident angle 0° and R(395, 60, 0.7, λ) at incident angle 40°.
(b)-reflectance spectrum of Japanese jewel beetle. From right to left, spectrums correspond to incident angles 20°, 30°, 40°, 50°, 60° respectively. R_1 and R_2 are selected as R(530, 110, 0.73, λ) at incident angle 10° and R(460, 110, 1, λ) at incident angle 60°.

The reference data are described in Figure 13. The data of morpho butterflies is derived from Sun`s physical simulation[11]. The other data is reflectance spectrum of Japanese jewel beetle measured by Stavenga[14]. Spectrum shift in proportion to incident angle is confirmed.

Incident angle dependency of reflectance spectrum is calculated by our method in Figure 14. The values (λ_{peaki}, w_i, h_i) of R_i and its corresponding θ_i (i=1,2) for calculation are (460, 70, 1) at 0°, (395, 60, 0.7) at 40° for morpho butterflies and (530, 110, 0.73) at 10°, (460, 110, 1) at 60° for Japanese jewel beetles. These R_1 and R_2 are measured from reference data in Figure 13.

From the comparison of our results and reference data, it can be said that angular dependency of spectrum by our method is sufficiently in accordance with the one by other groups.

5.2 Rendering Results

Rendering results of morpho butterfly and Japanese jewel beetle are depicted in Figure 15 and Figure 16. The values of R_1 and R_2 discussed in section 5.1 are used to render each object. The rendered images show color shifts(from cyan to violet for morpho butterfly and from green to violet for Japanese jewel beetle) that agree with the observed iridescences of them.

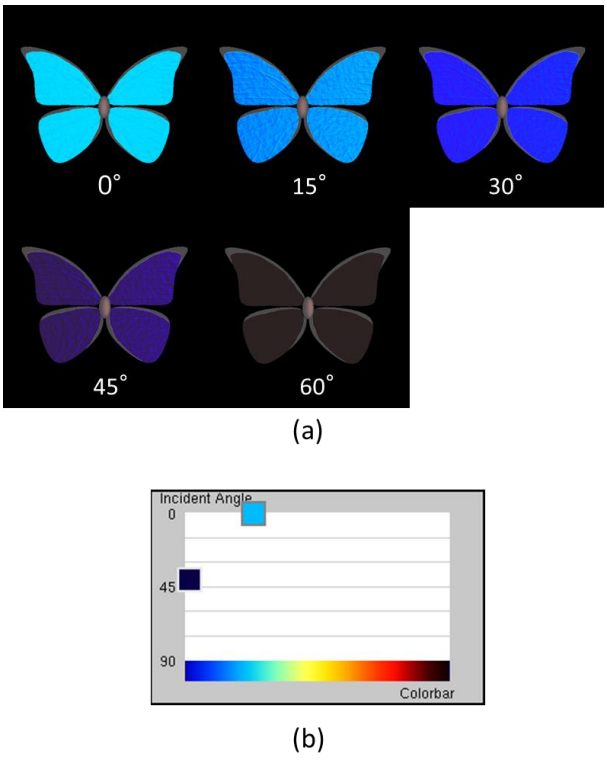

Figure 15 Rendering results of morpho butterfly
(a)-incident angles are described below each image.
(b)-λ_{peak}-θ plane setting for the rendering.

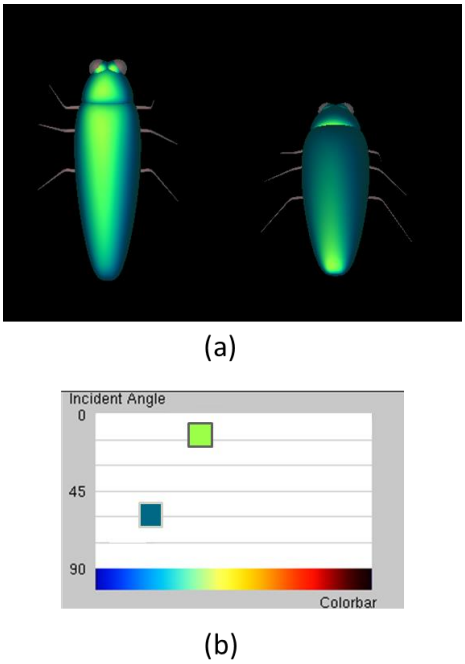

Figure 16 Rendering results of Japanese jewel beetle
(a)-rendering images of two different position.
(b)- λ_{peak}-θ plane setting for the rendering.

5.3 User Study

We conducted user study to compare usability of our system and the one of physical parameters input based system through measuring time to render given sample images of iridescences. The latter system was implemented based on Sun`s empirical model[11] for biological iridescences due to multilayer structure. In this system, to render iridescences, users are needed to input physical properties of surface such as thickness of film, thickness of air, index of refraction of film and one auxiliary parameter.

The protocol used in this study was as following.

1. 3 sample images, image 1, 2, 3(Figure 17) of iridescence are given to participants.

2. The Participants are required to render same images of the given samples using two systems above. Specifically, image 1, 2, 3 are rendered with one system in sequence, and then, these are rendered again with the other system. Time to get the same image was measured for each image.

8 participants (who are not familiar with iridescence phenomenon) were divided into 2 groups, A and B for this test. Participants of A group used our system first and the system based on Sun`s model later in part 2 of the protocol. Participants of B group tested systems in opposite order. The reason to divide two groups is to consider the influence of the order testing systems.

The result of user study is shown in Figure 18. In Figure 18, y axis means average time for each group A(represented as (A)) or B(represented as (B)) to get images using system based on Sun`s model( represented as Sun) or our system( represented as Park). X axis represents sample image number. From the results, it is obvious that the order of using system doesn`t influence results in that A group and B group shows similar results for the same system. In addition, it can be said that our color palette based user interface provides intuitive usability since average time to get images by our system are shorter than the one by the other system.

Figure 17 3 sample images of iridescences
From left to right, samples are image1, image2 and image3 respectively.

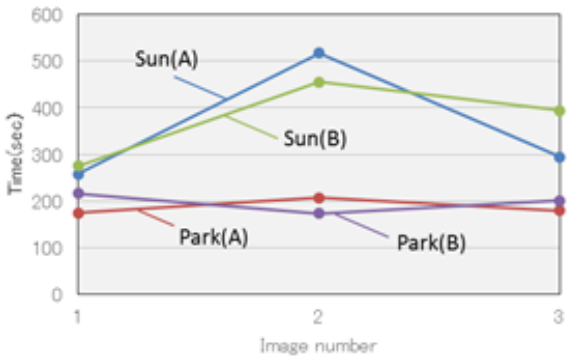

Figure 18 Results of user study

6 Conclusion

In this paper, we proposed a color palette based user interface for biological iridescences rendering.

This system allows users to pick two colors from color palette corresponding to their incident angles. From this information, two reflectance spectrums are defined and correspondence between reflectance spectrums and incident angles is calculated based on the two spectrums and equation of constructive interference.

We also evaluated our system in three points, reflectance spectrum validation, rendering results and user study. In reflectance spectrum comparison and rendering results, calculated spectrums and rendered images of morpho butterflies and Japanese jewel beetles based on our method matched well with both real spectrum data and real images. In user study, users rendered sample images with our new system and previous system(namely, physical parameters input based system), and it turned out that users can render aimed iridescences with shorter time when they used our system.

Even though our approach provides not only effective usability, but also physically sound rendering results, the method adopted in this paper is only for iridescences caused by biological multilayer system. As mentioned in section 1, since iridescences can occur through various mechanisms, further research should be carried out to achieve general usability covering such iridescences.

Appendix
Transformation of Spectrum to RGB

By using color matching function $x(\lambda)$, $y(\lambda)$, $z(\lambda)$(which is defined by the International Commission on Illumination(CIE)) and following equation(A.1), reflectance spectrum $R(\lambda)$ can be transformed to 3 standard primaries, X, Y and Z.

$$\begin{aligned} X &= k \int R(\lambda) x(\lambda) \mathrm{d}\lambda \\ Y &= k \int R(\lambda) y(\lambda) \mathrm{d}\lambda \\ Z &= k \int R(\lambda) z(\lambda) \mathrm{d}\lambda \end{aligned} \quad \text{(A.1)}$$

Integral range is from 380 to 780 and k is coefficient. Transforming XYZ to RGB is represented as equation(A.2)[15].

$$\begin{aligned} R &= 3.2406X - 1.5372Y - 0.4986Z \\ G &= -0.9689X + 1.8758Y + 0.0415Z \\ B &= 0.0557X - 0.2040Y + 1.0570Z \end{aligned} \quad \text{(A.2)}$$

References

[1] “Iridescence in Leopidoptera”, *Photonics in Nature*, University of Exter, 1998.

[2] 木下修一, *生物ナノフォトニクス　構造色入門*、朝倉書店、2010.(Japanese)

[3] Symposium on Structural Color, *http://mph.fbs.osaka-u.ac.jp/*

[4] Kinoshita, S., Yoshioka, S., Fujii, Y., Okamoto, N, *Photophysics of Structural Color in the MorphoButterflies*, Forma, Vol.17, pp. 103-121, 2002

[5] Hirayama, H., Yamaji, Y., Kaneda, K., Yamashita, H., Y. Monden Y., *Rendering Iridescent Colors Appearing on Natural Objects*, PG` 00 Proceedings of the 8th Pacific Conference on Computer Graphics and Applications, page 15, 2000

[6] Hirayama, H., Kaneda, K., Yamashita, H., Monden, Y., *An Accurate illumination model for objects coated with multilayer films*, Computer&Graphics, Volume 25, Issue 3, pp. 391-400, 2001

[7] Joe Stam, *Diffraction shaders*, SIGGRAPH99, pp. 101-110, 1999

[8] Gondek, J. S., Meyer, G. W., Newman, J. G., *Wavelength dependent reflectance functions*, In Proceedings of ACM SIGGRAPH94, pp. 213-220, 1994

[9] Shun Iwasawa, Naohiro Shichijo, Yoichiro Kawaguchi, *Rendering Methods for Models with Complicated MicroStructures*, ICAT, 2004

[10] Noriko Nagata, Toshimasa Dobashi, Yoshitsugu Manabe, Teruo Usami, Seiji Inokuchi, *Modeling and Visualization for a Pearl-Quality Evaluation Simulator*, IEEE Transactions on Visualization and Computer Graphics, Vol. 3, Issue 4, pp. 307-315, 1997

[11] Yinlong Sun. *Rendering Biological Iridescences with RGB-Based Renderers*, ACM Transactions on Graphics, Vol. 25, No. 1, pp. 100-129, 2006

[12] Land, M. F., *The physics and biology of animal reflectors*, Prog. Biophys. Mol. Biol. 24, p. 78, 1972

[13] Eugene Hecht, *ヘクト光学*, 丸善, 2003

[14] Stavenga DG, Wilts BD, Leertouwer HL and Hariyama, *Polarized iridescence of the multilayered elytra of the Japanese Jewel Beetle, Chrysochroa Fulgidissima*, Philosophical Transanctions of the Royal Society, B 366: 709-723, 2011

[15] International Color Consortium, *http://www.color.org/*